Using DCE-MRI model selection to investigate the disrupted microvascular charateristics of tumour-bearing livers

A. Banerji[1,2], J. H. Naish[1,2], Y. Watson[1,2], G. A. Buonaccorsi[1,2], and G. J. Parker[1,2]

[1]Imaging Sciences and Biomedical Engineering, School of Cancer and Imaging Sciences, The University of Manchester, Manchester, United Kingdom, [2]Biomedical Imaging Institute, Manchester, United Kingdom

Introduction Dynamic contrast-enhanced (DCE) MRI allows us to probe the microvascular characteristics of different tissue types, and is increasingly used in clinical trials of anti-angiogenic agents, for example in liver tumours. Healthy liver tissue has a dual blood supply from the hepatic artery and hepatic portal vein. The smallest vascular structures in the liver that eventually receive blood from both supplies are the sinusoids, whose fenestrated walls and lack of basement membrane allow the contents of the plasma to easily wash out of the vasculature. In comparison, tumours recruit predominantly an arterial blood supply and contain capillaries that can have a more restrictive vascular wall structure than sinusoids. Global changes to the hepatic blood supply also occur because the tumour produces vasoactive agents that increase the resistance in the gastro-intestinal tract vasculature and this results in a decreased contribution from the portal vein. In this work we have investigated the disruption to the microvascular characteristics caused by disease by performing model selection using the Akaike selection criterion[1] to compare a novel implementation of a one-compartment, dual-input model that reflects healthy liver characteristics (the Materne model[2]) and a two-compartment single-input model that should better represent tumour (the extended Kety model[3]).

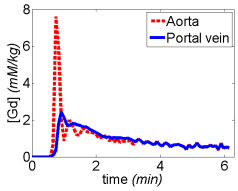

Fig 1. A measured AIF with the generated portal input function.

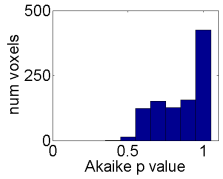

Fig 2. Akaike p values for synthetic data generated using the Materne model. 0 = extended Kety model; 1 = Materne model.

Methods An estimate of the portal input function is required for fitting the Materne model. However, accurate measurements are often problematic due to breathing motion, partial volume effects, signal contamination from the hepatic artery, and the absence of the portal vein from the field of view. We have developed a method for generating a portal input function from the patient's measured arterial input function (AIF). A reference portal input function from a CT data set[4] is deconvolved from a reference AIF from the same data set to give an impulse response function (IRF) relating the two input functions. The IRF is then applied to each acquired AIF to give a patient specific portal input function as shown in Fig. 1. This method was shown to produce plausible portal input functions by comparing generated portal input functions to those measured using an optimised protocol[5]. To validate the model selection, synthetic data was generated using the Materne model with a range of parameter values that correspond to healthy and cirrhotic liver states[6]. The population-averaged AIF[7] was used with a portal input function generated from this AIF as described above. 100 synthetic data sets were created with zero mean Gaussian noise added with a signal to noise ratio (SNR) of 10. The mean Akaike p value for the 100 data sets was calculated. The model selection was applied on a per voxel basis to 6 pre-treatment DCE-MRI patient data sets (acquired for clinical trials of anti-angiogenic agents with a temporal resolution of 4.97s with free breathing allowed). Three regions of interest were defined: the tumour; a 2 voxel shell around the tumour separated from the tumour by a voxel width; and an independently defined patch of liver tissue that attempts to avoid any tumour tissue or major vessels.

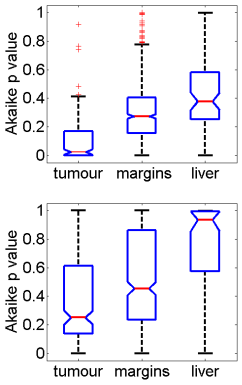

Fig 3. Akaike p values for 3 ROIs in patient 4 (top) and patient 2 (bottom). 0 = extended Kety model; 1 = Materne model.

Results Applying model selection to synthetic data generated with the Materne model demonstrates that the Materne model more accurately describes the concentration time curves in the majority of parameter combinations at this SNR (see Fig. 2). The preference for the Materne model is less clear at parameter combinations where the arterial fraction is high and the mean transit time is low. Fig. 3 shows the Akaike p values for the three ROIs for patient 4 and patient 2. The median p values between each of the three ROIs are found to be significantly different at the 1% level using the Mann-Whitney U-test. (For patient 2, these are: tumour – tumour margins p= 5.84×10^{-8}; tumour – liver p= 6.12×10^{-11}; tumour margins – liver p= 1.05×10^{-6}). The trend of increasing median p value from the tumour to the liver ROI is seen in all six patients. The difference in the median Akaike p value between the ROIs is significant at the 1% level in 5 of the 6 patients. However, only two patients have median p values for the liver ROI that correspond to selecting the Materne model. Fig. 4 shows a map of Akaike p values for patient 2. The tumours (shown by the arrows) can clearly be seen as dark patches (indicating selection of the extended Kety model) in the lighter coloured liver (indicating selection of the Materne model).

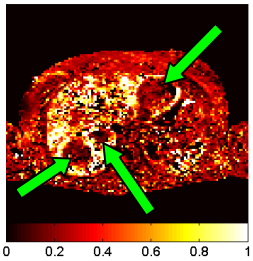

Fig 4. Akaike p value map for patient 2. 0 = extended Kety model; 1 = Materne model.

Conclusion Model selection using the Akaike selection criterion was performed to identify the spatial changes in microvascular characteristics in livers containing tumours. Validation of the selection process using synthetic data shows that the two models are distinguishable at a relevant noise level. Results from six patient data sets demonstrate that the extended Kety model is more appropriate within tumours than the Materne model and that the model selection shifts towards the Materne model as we move from a ROI in the tumour to a ROI in non-tumour liver tissue. This has application to the identification of tumours in the liver and for partial volume related errors.

References [1] Akaike, H., Automatic Control, IEEE Transactions on, 2003. 19(6): p. 716-723.
[2] Materne, R., et al., Clin Sci (Lond), 2000. 99(6): p. 517-525. [3] Tofts, P., Journal of Magnetic Resonance Imaging, 1997. 7(1): p. 91-101.
[4] Pandharipande, P., et al., Radiology, 2005. 234(3): p. 661-673. [5] Horsfield, M., et al., Physics in Medicine and Biology, 2009. 54(9): p. 2933-2949.
[6] Van Beers, B., et al., Am. J. Roentgenol., 2001. 176(3): p. 667-673. [7] Parker, G., et al., Magnetic Resonance in Medicine, 2006. 56(5): p. 993-1000.